Effects of Hydraulic Loading History on Suffusion Susceptibility of Cohesionless Soils

Abdul Rochim, Didier Marot, Luc Sibille, Van Thao Le

Rochim A., Marot D., Sibille L., Le V.T. (2017). Effect of hydraulic loading history on the characterization of suffusion susceptibility of cohesionless soils. Journal of Geotechnical and Geoenvironmental Engineering (ASCE), 143(7). DOI 10.1061/(ASCE)GT.1943-5606.0001673

Effects of hydraulic loading history on suffusion susceptibility of cohesionless soils

By Abdul ROCHIM[1,2], Didier MAROT[3], Luc SIBILLE[4], Van Thao LE[5,6]

[1] Dr. Abdul Rochim
Université de Nantes, Institut de Recherche en Génie Civil et Mécanique, CNRS
58 rue Michel Ange, BP 420
F-44606 Saint-Nazaire Cedex, France
[2] Civil Engineering Department, Sultan Agung Islamic University,
Indonesia
Email : abdoul.rochim@etu.univ-nantes.fr

[3] Prof. Didier Marot
Université de Nantes, Institut de Recherche en Génie Civil et Mécanique, CNRS
58 rue Michel Ange, BP 420
F-44606 Saint-Nazaire Cedex, France
Email : didier.marot@univ-nantes.fr

[4] Dr. Luc Sibille
Université Grenoble Alpes, CNRS, 3SR,
F-38000 Grenoble, France
Email : luc.sibille@3sr-grenoble.fr

[5] Van Thao Le, Ph.D student
Université de Nantes, Institut de Recherche en Génie Civil et Mécanique, CNRS
58 rue Michel Ange, BP 420
F-44606 Saint-Nazaire Cedex, France
[6] University of Science and Technology –The University of Danang
54 Nguyen Luong Bang Street, Lien Chieu District, Da Nang city, Vietnam
Email: van-thao.le@etu.univ-nantes.fr

Corresponding author: Didier Marot
Tel: 33 2 40 17 81 89 Fax : 33 2 40 17 81 60
Email: didier.marot@univ-nantes.fr

35

Abstract

37 Suffusion is a selective erosion of fine particles under the effect of seepage
38 flow within the matrix of coarser particles. This complex phenomenon appears as a
39 combination of three processes: detachment, transport and possible filtration of
40 finer fraction. It can induce a change in particle size distribution, porosity and
41 hydraulic conductivity of the material. With the objective to characterize the
42 suffusion susceptibility, downward seepage flow tests were conducted. Four
43 different cohesionless soils were tested under hydraulic gradient controlled
44 conditions or under flow rate controlled conditions. This study shows the significant
45 effect of hydraulic loading history on the value of critical hydraulic gradient.
46 Moreover, method characterizing the erosion susceptibility based on rate of erosion
47 does not lead to a unique characterization of suffusion process for different types
48 of hydraulic loading. The new analysis is based on energy expended by the
49 seepage flow and the cumulative eroded dry mass. The results demonstrate that
50 this approach is more effective to characterize suffusion susceptibility for
51 cohesionless soils.

52 **Key words :** Dam safety – Cohesionless soils – Erodimeter – Suffusion – Water
53 seepage energy

54

INTRODUCTION

Hydraulic earth structures can suffer from instabilities induced by internal erosion processes. Fry et al. (2012) indicated that overtopping and internal erosion are the two main causes of failure of embankment dams and dikes.

Fell and Fry (2013) distinguished four forms of internal erosion: concentrated leak erosion, backward erosion, contact erosion and suffusion. This paper deals with suffusion which can induce a change in particle size distribution, porosity and hydraulic conductivity of the soil. Moreover, although the suffusion development may be difficult to detect in situ, it has to be considered with attention as it can evolve towards a second phase of erosion, characterized by a blowout and an extensive erosion of fine particles, inducing both a large settlement of specimen and a relatively strong increase in the hydraulic conductivity (Sibille et al., 2015a). Thus to ensure the safety assessment of hydraulic earth structures, the characterization of suffusion susceptibility is required. Nevertheless, it was only recently that a method for classifying the suffusion susceptibility of soils based on experimental results was proposed (Marot et al., 2016).

Soils that are likely to suffer from suffusion, have a grain-size distribution curve either discontinuous or upwardly concave (Fell and Fry, 2007), and even with a slight variation of the initial gradation, an abrupt transition appears between internally stable and unstable states (Skempton and Brogan, 1994).

It is worth stressing that in comparison with time scale in laboratory, in-situ the hydraulic loading can be applied on soils, constituting the hydraulic earth structures and its foundations, during a very long duration. The upstream head applied on an earth structure can increase by several cm per hour in case of flood, a rapid reservoir

filling or heavy rain seasons, but only a few mm per day under normal flow conditions. The corresponding values of increment of hydraulic gradient depend on the earth structure's design and also on the studied position in this structure. Moreover the seepage flow depends on aforementioned parameters but also on hydraulic conductivity of soils. Thus to optimize the test duration and to take into account this large range of possible hydraulic loadings, researchers performed internal erosion tests under various hydraulic loading conditions. Suffusion tests described in literature, were mostly performed under multi-staged hydraulic gradient conditions in upward direction with hydraulic gradient ranging from 0.02 to 1.4 (Skempton and Brogan, 1994; Ke and Takahashi, 2012; Indraratna et al., 2015) or in downward direction with the hydraulic gradient range from 0.15 to 9.4 (Moffat and Fannin, 2006; Chang and Zhang, 2011). But other tests were also realized under single staged hydraulic gradient with values between 5 and 140 (Bendahmane et al., 2008; Wan and Fell, 2008; Nguyen et al., 2012). Nguyen et al. (2012) and Ke and Takahashi (2014, 2015) performed suffusion tests under flow rate controlled conditions with a range of discharge per unit cross section from 10^{-3} to 0.13 $cm.s^{-1}$. Kenney and Lau (1985) described their test conditions as severe because the values of discharge per unit cross section were larger than those usually encountered in engineering practice with similarly graded materials (0.37 to 1.67$cm.s^{-1}$). However, facing this variability of hydraulic loading conditions, no clear influence on suffusion susceptibility of hydraulic loading history could be drawn. Even with the same type of hydraulic loading (i.e. hydraulic gradient controlled conditions) Luo et al. (2013) showed that for the tested soil, the suffusion susceptibility seems to be influenced by the increment of hydraulic gradient and by the duration of each stage. This soil appears more resistant when

facing suffusion process in the “short-term experiment” (multi-staged hydraulic gradient with increment ranging from 0.06 to 0.54 and with stage duration from 10 to 30 min) than that in the “long-term large hydraulic head experiment” (large single staged hydraulic gradient remained constant up to eight days).

The main objective of this paper is to investigate (1) the suffusion susceptibility of gap and widely graded soils showing a slight variation of the initial gradation, and (2) the hydraulic loading history effects on this susceptibility. A series of downward seepage flow tests was realized under hydraulic gradient and flow rate controlled conditions. Moreover different increments of hydraulic gradient, different flow rates and different test durations were used. The results are discussed in terms of gradation of suffusion susceptibility. Hydraulic loading history effects on the value of critical hydraulic gradient and on the rate of erosion are studied. Finally the suffusion susceptibility is also assessed by a new energy based method and recommendations for suffusion tests are given.

CONTROL PARAMETERS FOR LIKELIHOOD OF SUFFUSION

Three criteria are distinguished for suffusion to occur (Fell and Fry, 2013): (i) the size of the fine soil particles must be smaller than the size of the constrictions between the coarser particles, which form the basic skeleton of the soil. (ii) The volume of fine soil particles must be less than the volume of voids between coarser particles, and (iii) the velocity of flow through the soil matrix must be high enough to move the loose fine soil particles through the pore. The first two criteria are associated with the fabric of granular soils, which mainly depends on the grain size distribution. Thus to assess the potential susceptibility of a soil to suffusion, several researchers proposed methods that are only based on the study of soil gradation (US Army Corps of Engineers, 1953;

Kenney and Lau, 1985; Li and Fannin, 2008; Chang and Zhang, 2013 among others). However, the modification of the effective stress (Moffat and Fannin, 2006; Bendahmane et al. 2008; Chang and Zhang, 2011) and the relative density (Indraratna et al., 2015) can also influence the suffusion susceptibility. Finally, for a given grain size distribution and a given value of effective stress, angularity of coarse fraction grains contributes to increase the suffusion resistance (Marot et al., 2012). The third criterion is related to the action of the fluid phase with respect to seepage loading required to detach and then to transport the fine particles. Skempton and Brogan (1994), Ke and Takahashi (2012), Indraratna et al. (2015) proposed to relate the onset of suffusion with an increase of hydraulic conductivity. Skempton and Brogan proposed to characterize the corresponding hydraulic loading by the critical hydraulic gradient. However a fraction of the detached particles can re-settle or be filtered at the bulk of the porous network (Reddi et al. 2000; Bendahmane et al. 2008; Marot et al. 2009; 2011a; Nguyen et al. 2012; Luo et al., 2013). These processes can eventually induce local clogging, accompanied by variations of fluid velocity and interstitial pressure. Therefore, variations of both seepage flow and pressure gradient have to be taken into account to evaluate the hydraulic loading. By considering these both parameters, Reddi et al. (2000) assumed that hydraulic loading can be represented by the viscous shear stress at fluid-solid interface. They expressed this shear stress, τ, for a horizontal flow in the porous medium, and it can be reformulated for a vertical flow by:

$$\tau = \left(\frac{\Delta h \, \gamma_w}{\Delta z} \right) \frac{r}{2} \qquad (1)$$

where Δh is the drop of hydraulic head between upstream section A and downstream section B, γ_w is the unit weight of water, $\Delta z = z_A - z_B$, z_A and z_B are altitudes of sections A and B respectively. The equivalent radius, r, is representing the effects of all pores. In the case of cohesive soils, Reddi et al. (2000) proposed to estimate the equivalent radius of pores by:

$$r = \sqrt{\frac{8\,k\,\eta}{n\,\gamma_w}} \tag{2}$$

where n is the porosity, k is the hydraulic conductivity and η the dynamic viscosity. Consequently, the hydraulic shear stress along vertical system of capillary tubes can be expressed by:

$$\tau = \left(\frac{\Delta h}{\Delta z}\right)\sqrt{\frac{2\,k\,\eta\,\gamma_w}{n}} \tag{3}$$

For erodibility characterization, a commonly used interpretative method for hole erosion tests (Wan and Fell, 2004) consists in describing the erosion rate from the excess shear stress equation, defined by:

$$\dot{m} = k_d\,(\tau - \tau_c) \qquad \text{for } \tau \geq \tau_c \tag{4}$$

where k_d is the erosion coefficient, and τ_c is the critical hydraulic shear stress. The considered soil-water interface is the hole surface which is assumed to be cylindrical. Reddi et al. (2000) considered that the surface of pores is more representative for suffusion process, thus they expressed the erosion rate of soils per unit pore ($\dot{m}$) by:

$$\dot{m} = \frac{m(\Delta t)}{N_p\,S_p\,\Delta t} \tag{5}$$

where m is eroded dry mass during the elapsed time Δt, N_p the number of average pores, and S_p the average pore area. Assuming an equivalent pore radius r as defined in Eq.2, N_p and S_p can be computed respectively by:

$$N_p = \frac{S\,n}{\pi\, r^2} \tag{6}$$

$$S_p = 2\,\pi\, r\, L \tag{7}$$

where S is the cross section area of the specimen and L is the length of the specimen.

Another way to consider variations of both seepage velocity and pressure gradient, consists in expressing the power expended by the seepage flow (Marot et al., 2011b; Marot et al., 2016). Three assumptions are used: the fluid temperature is assumed constant, the system is considered as adiabatic and only a steady state is considered. The energy conservation equation permits to express the total flow power as the summation of the power transferred from the fluid to the solid particles and the power dissipated by viscous stresses in the fluid. As the transfer between fluid and solid appears negligible in suffusion process (Sibille et al., 2015b), the authors suggest to characterize the fluid loading from the total flow power, P_{flow} which is expressed by:

$$P_{flow} = Q\,\gamma_w\,\Delta h \tag{8}$$

where Q is the fluid flow rate.

Marot at al. (2011b) expressed the erosion resistance index by:

$$I_\alpha = -\log\left(\frac{m_{dry}}{E_{flow}}\right) \tag{9}$$

where E_{flow} is the expended energy, computed by time integration of the instantaneous flow power, and m_{dry} is the cumulative eroded dry mass. From this energy based

189 method, six categories of suffusion soil sensibility are proposed: from highly resistant
190 to highly erodible (Marot et al., 2016).

191 LABORATORY EXPERIMENTS

192 Main characteristics of testing apparatus

193 The device is designed to apply downward seepage on fine soil specimens (50 mm in
194 diameter and heights up to 100 mm) (Fig. 1). The hydraulic gradient of this seepage
195 is controlled thanks to an injection cell equipped with pressure sensor, and connected
196 to an air/water interface cylinder. The system to generate seepage flow in flow-rate-
197 controlled conditions comprises a gear pump connected to a pressure sensor at its
198 outlet. The fluid passes through the top cap which contains a layer of glass beads to
199 diffuse the fluid uniformly on the specimen top surface. The funnel-shaped draining
200 system is connected to an effluent tank by a glass pipe. The effluent tank is equipped
201 with an overflow outlet (to control the downstream hydraulic head) and a rotating
202 sampling system containing 8 beakers for the sampling of eroded particles carried with
203 the effluent. In the case of clay or silt suffusion, a multi-channel optical sensor can be
204 placed around the glass pipe (Marot et al., 2011a), and thanks to a preliminary
205 calibration, clay or silt concentration in the effluent can be computed. At the overflow
206 outlet of the effluent tank, water falls in a beaker which is continuously weighed in
207 order to determine injected flow rate. The sample is supported by a lower mesh screen
208 and the mesh screen opening size is selected with the objective to reproduce in-situ
209 earth structures without filter, as a dike for example.

Testing materials

Three gap graded soils and one widely graded soil, composed of sand and gravel were tested. A laser diffraction particle-size analyser was used to measure the grain size distribution of these soils (Fig. 2). Tests were performed with demineralised water and without deflocculation agent. Table 1 summarizes the properties of soils used in the laboratory tests. These soils were selected in order to obtain internally unstable soils. Their gradations slightly differ, mainly with respect to the fine content ranging from 20% to less than 30% (Fig. 2). According to grain size based criteria these soils are, indeed internally unstable, but close to the stability limits defined by several methods currently available and detailed hereafter. For all studied soils, the uniformity coefficient C_u is around 20 (i.e. the stability boundary proposed by US Army Corps of Engineers, 1953). Minimum values of Kenney and Lau's (1985) ratio (H/F) are lower than 1 for all tested soils, thus according to this criterion, they are considered as internally unstable. As the percentage of fine P is smaller than 5%, and the gap ratio G_r is higher than 3, Chang and Zhang's (2013) method assessed widely graded soil R and gap graded soils A, B, C as internally unstable. However, G_r value for soils A and B, is slightly higher than 3, corresponding to the stability boundary proposed by Chang and Zhang. The method proposed by Indraratna et al. (2015) combines the particle size distribution and the relative density. In Table 1 values of ratio $D_{c35}^{c}/d_{85,SA}^{f}$ were computed with the highest value of specimen initial dry density discussed later in this paper. According to this method, all specimens are considered to be internally unstable.

Specimen preparation and testing program

The specimen preparation phase is divided into three steps: production, installation and then saturation of the specimen. The repeatability of the production is achieved by the following procedure. First sand grains and gravel are mixed with a moisture content of 7.8%. To prepare these specimens, a single layer semi-static compaction technique is used, until the initial fixed dry density is reached with 50 mm specimen height. Two values of initial dry density are targeted: 90% and 97% of the optimum Proctor density. As recommended by Kenney and Lau (1985), in order to reduce preferential flow, each specimen is wrapped in a latex sleeve, then put inside a metal mould. The downstream filter is composed of a 4 mm pore opening grid. Such a pore opening allows the migration of all sand particles as in the case of earth structures without any filter. The saturation phase begins with an upward injection of carbon dioxide during 5 minutes to improve dissolution of gases into water, afterwards demineralized water is injected under low hydraulic gradient. The saturation process takes twelve hours until water trickles over the top cap. With this preparation technique (Nguyen, 2012), the final saturation ratio was determined by measuring density and water content and reached 95%. Finally, the specimen is subjected to a downward flow, using demineralized water and three kinds of hydraulic loading. The choice of these hydraulic loading programs constitutes a compromise between hydraulic loadings representative of real hydraulic conditions in the field, and the possibility to characterize the sensibility of a soil to suffusion in a couple of hours. Test duration is indeed decisive from an engineering point of view, in particular during an earth structure construction. Figure 3 shows the time evolution of the applied hydraulic gradients. Multi-staged hydraulic gradients represent different increases of hydraulic

256 loading which are more or less severe. First multi-staged hydraulic gradient condition
257 (named a) consists of increasing the hydraulic gradient by steps of 0.1 until 2, then by
258 steps of 0.5 between 2 and 4 and by steps of 1 beyond. For the second kind of
259 hydraulic loading (b), hydraulic gradient increment is directly equal to 1. For both
260 hydraulic loadings, each stage of hydraulic gradient is kept constant during 10 min.
261 For hydraulic loading (k) with hydraulic gradient increment of 0.5, the duration of
262 hydraulic gradient stage is 12 hours. Hydraulic loading (c) represents a constant
263 hydraulic gradient of 4 in order to represent the constant hydraulic head occurring for
264 instance in the cases of large reservoirs or canals during normal flow conditions. For
265 this type of hydraulic loading the hydraulic gradient is voluntary chosen quite high to
266 try to force the occurrence of suffusion (this point is based on the a priori assumption,
267 but not always verified a posteriori, that the higher the hydraulic gradient is the more
268 suffusion is prone to occurring). Finally with the objective to recreate the same
269 hydraulic loading condition as used by Kenney and Lau (1985), Nguyen et al. (2012)
270 and Ke and Takahashi (2014, 2015) in their suffusion tests, two constant flow rates
271 are used (q1=1.247 ml.min^{-1} and q2=1.641 ml.min^{-1}, corresponding value of discharge
272 per unit cross section 10^{-3} cm.s^{-1} and 1.4 10^{-3} cm.s^{-1} respectively).

273 With the objective to improve the readability, the first letter of each test name is related
274 to the gradation (Fig. 2), the last letter indicates the type of hydraulic loading type and
275 the number details the initial relative density. Table 2 indicates the initial dry density of
276 sixteen tested specimens, the values of applied hydraulic gradient or injected flow rate
277 and the duration for each test.

The repeatability of tests was verified by performing 2 tests under identical conditions: A-a and A-a_rep.

RESULTS AND DISCUSSION

Hydraulic behavior of tested specimens

The hydraulic conductivity of tested specimens are shown on Fig. 4 and Fig. 5 in the case of hydraulic loadings (a) and (b). For these types of hydraulic loadings, the hydraulic conductivity first decreases with a kinetic depending on the hydraulic loading type and also on the relative density. In the case of hydraulic loading (b), the duration of this first decreasing step is from 10 min (tests C-b, B97-b, R90-b) to 20 min (tests A-b, R97-b). Whereas under hydraulic loading (a), the hydraulic conductivity decreases for a much longer time (50 min for test R90-a; 80 min for test B90-a; 120 min for tests A-a, A-a_rep, C-a and even 150 min for B97-a). For a given gradation and a given hydraulic loading, this decreasing phase is longer for a denser specimen (for example: R90-b in comparison with R97-b; and B90-a in comparison with B97-a). The second phase of hydraulic conductivity evolution is characterized by a rapid increase by a factor between 4 (test A-b) and 20 (test A-a_rep). Finally the hydraulic conductivity reaches a constant value which is pointed out by black spots on Fig. 4 and Fig. 5. The repeatability of the seepage test can be validated by comparing the initial and final values of hydraulic conductivity for tests A-a and A-a_rep which are in good agreement. However, irregular deviation of hydraulic conductivity appears in the middle of test. Only a few data exist in literature concerning suffusion test repeatability. Ke and Takahashi (2014) observed same hydraulic conductivity deviation which they attributed to the difference in homogeneity among the reconstituted soil specimens. In

addition the complexity of suffusion process, highlighted by the identification of predominant processes discussed in the following section may explain the deviation of hydraulic conductivity evolution during the suffusion development.

Figure 6 shows the slow and monotonous decrease with time of the hydraulic conductivity which is measured during single staged hydraulic gradient tests (tests A-c, B90-c, and test B90-k during the first hydraulic stage with a duration of 720 min) or under flow rate controlled tests (tests B90-q2 and R97-q1). Thus some variations in the hydraulic loading appear necessary in order to initiate the second increasing phase of the hydraulic conductivity, even after several hours of seepage as during test B90-k (Fig. 3).

Identification of predominant processes

The comparison of time evolution of hydraulic conductivity with time evolution of erosion rate and measurement of post suffusion-test soil grading constitute a way to improve the understanding of suffusion process.

Figure 7 shows the erosion rate per unit pore area (computed by Eq. 5) for tests B90-a, c, q2. The erosion rate is depending on hydraulic conductivity and porosity, which evolve in time. For the computation of porosity during time, the specimen height is assumed constant and the eroded mass measurement is taken into account.

The decrease of hydraulic conductivity is systematically accompanied by a decrease of erosion rate, which suggests that some detached particles can be filtered within the soil itself. This filtration may induce a clogging of several pores followed by a decrease of the hydraulic conductivity. Under multi staged hydraulic gradient conditions, a rough

increase of the erosion rate occurs simultaneously with the increase of the hydraulic conductivity. These simultaneous increases confirm that a clogging firstly restricting the water flow can be blown away by a sudden increase of the hydraulic loading. Thus the predominant process during this second phase seems to be the detachment and transport of solid particles. Finally hydraulic conductivity tends to stabilize while the erosion rate decreases. This third phase could be explained by the presence of preferential flows created by the erosion process leading to a steady state.

At the end of suffusion tests A-a and B90-a, specimens were divided in two parts named upstream and downstream parts and their grain size distributions were measured. Figures 8(a) and 8(b) show the initial gradation and the gradation of downstream and upstream parts of soils A and B respectively. For both specimens, it can be noted that the loss of fine particles is higher in the upstream part. This result is in agreement with results of Ke and Takahashi (2012). The transport of detached particles from upstream to downstream parts can partly offset the loss of particles in the downstream part. Moreover in downstream part of specimen A, the final percentage of fine exceeds the initial percentage, which confirms the process of filtration. In the upstream part, the percentage of fine particles corresponds only to half of the initial fine percentage of specimen A, whereas it represents about 80% of the initial fine percentage in specimen B. Thus filtration process appears to be raised by the amount of detached particles which come from the upstream part. Furthermore specimens A and B90 have the same initial density (see Table 2), but different percentage of fine. For a given density, a lower fine content is accompanied with a larger amount of coarse particles and a smaller constriction size within the porous network, which facilitates the filtration process.

It is worth noting that for a given soil, a multi staged hydraulic loading with higher increments induces a higher final value of hydraulic conductivity. Final hydraulic conductivity is higher under hydraulic loading (b) than under hydraulic loading (a) (tests A-a, A-a_rep, A-b, R90-a and R90-b on Fig. 4 and tests B97-a, B97-b, C-a and C-b on Fig. 5) and also higher than in the case of hydraulic loading (k) (test B90-a on Fig. 5 and test B90-k on Fig. 6). Thus an application of higher increments may limit the filtration process.

The loading by multi staged hydraulic gradient which was applied for test B90-a permits to obtain the three aforementioned phases and the steady state which follows an extensive erosion is reached for i=4 (Fig. 5). This same value of hydraulic gradient i=4 was continuously applied during test B90-c, but this hydraulic loading leads only to the predominant process of filtration (Fig. 6). Therefore, the history for reaching that final hydraulic gradient has a significant influence on the hydraulic behavior of specimens and on the development of suffusion.

Finally, the complex erosion phenomenon of suffusion appears as a combination of three processes: detachment, transport and possible filtration of finer fraction. This combination results in strong heterogeneities in soil grading and large evolutions of hydraulic conductivity and erosion rate. The development of these coupled processes depends on the grain size distribution, the density but also the evolution of hydraulic loading which in turns is influenced by the suffusion development.

Characterization of suffusion onset

Figure 9 shows the flow velocity versus the hydraulic gradient for tests on soil B. With the objective to determine with accuracy the onset of suffusion, the relative evolution

of hydraulic conductivity is computed and the onset of suffusion is systematically defined by the first relative increase of 10%. First, it can be observed that under single staged hydraulic gradient conditions and under flow rate controlled conditions (tests B90-c and B90-q2 respectively, on Fig. 9), the determination with such approach of the suffusion onset is not possible. For tests realized under multi staged hydraulic gradient conditions, the values of the critical hydraulic gradient are indicated in Table 3. The critical hydraulic gradient appears higher with the hydraulic loading (b) than with the hydraulic loading (a) for soils A, B97 and R90. In consequence, for a given soil the critical hydraulic gradient seems to depend on the history of hydraulic loading. This influence of hydraulic loading history was also observed by Luo et al. (2013) who compared the results obtained with two test durations. They notably concluded that a long-term large hydraulic head reduces the hydraulic gradient needed for major suffusion development.

For both hydraulic loadings, the comparison of critical hydraulic gradient obtained for tested soils shows that soil A requires a larger hydraulic gradient to initiate the suffusion process. The initial gradation of this soil has a lower fine content (20%) in comparison with soil B (initial fine content of 25%), and soils C and R (initial fine content about 29%). These results are in good agreement with the test results presented by Ke and Takahashi (2012) on cohesionless soils with three different initial fine contents from 16.7% to 25%.

Characterization of suffusion development

As for other internal erosion processes, a first interpretative method for suffusion tests could consist in representing the erosion rate as a function of the hydraulic shear stress. As for erosion rate computation (Eq. 5), the computation of hydraulic shear

stress (Eq. 3) takes into account the time evolutions of hydraulic conductivity and porosity. Value of porosity corresponds to an average value which characterizes the whole specimen, without distinction between upstream and downstream parts. However, thanks to the hydraulic conductivity evolutions, Eq. 3 takes partially into account the development of specimen heterogeneities during experiment time.

Figure 10 shows the erosion rate versus the hydraulic shear stress for tests on soil A. Thanks to the aforementioned identification of suffusion onset, based on hydraulic conductivity increase, it is possible to define the initiation of suffusion development phase. The end of this phase is assumed to be reached at the stabilization of the hydraulic conductivity. Now by considering only tests realized under hydraulic loadings (a) and (b), a linear approximation representing Eq. 4 is computed. Figure 10 shows the corresponding equation with values of k_d, τ_c and correlation coefficient R^2 for tests A-a, A-a_rep and A-b. The erosion rate versus the hydraulic shear stress are basically close for tests A-a, A-a_rep which might imply the good repeatability of the suffusion test. Table 4 details the values of erosion coefficient and correlation coefficient for tested specimens under multi staged hydraulic gradient conditions. First, it is worth noting the weak values of correlation coefficient (between 0.01 for test B97-a, and 0.77 for test A-a) highlighting the difficulty to describe the erosion rate from this approach. These low values of correlation coefficient cannot be attributed to the imprecision of the determination of erosion rate and hydraulic shear stress which can be valued at $\pm 3\ 10^{-11}$ kg.s^{-1}.m^{-2} and ± 0.02 Pa respectively. Moreover, the erosion coefficient values obtained with hydraulic loading (b) are systematically higher (with a factor between 1.4 and 3.3) than in the case of hydraulic loading (a). Thus the characterization of suffusion susceptibility based on this interpretative method

depends on the history of hydraulic loading. Moreover, in the case of flow rate controlled condition tests or single staged hydraulic gradient tests (A-c on Fig. 10) and even under hydraulic loading (k), a single value of hydraulic shear stress can be associated with a large range of erosion rate. In consequence, it is not possible to describe with accuracy the erosion rate by such interpretative method.

With the objective to take into account the history of hydraulic loading, the energy expended by the seepage flow E_{flow} is determined by the time integration of total flow power, P_{flow} (computed by Eq. 8) for the test duration. Figures 11 to 14 show the cumulative loss dry mass, m_{dry}, versus the cumulative expended energy for all kinds of hydraulic loading.

For characterizing the erosion susceptibility, the erosion resistance index is computed at the end of the test which is determined by the stabilization of the hydraulic conductivity, pointed out by black spots on Figures 11 to 14. If the test is stopped before the stabilization of the hydraulic conductivity, the erosion resistance index is computed with the last realized measurements. Table 5 indicates the values of erosion resistance index for all realized tests.

It is worth noting that when the stabilization of the hydraulic conductivity is reached, the corresponding value of erosion resistance index, written in bold in Table 5, can be determined with accuracy for the different hydraulic loadings. I_α is between 3.40 and 3.64 for tests B97 (i.e. this soil is moderately erodible according to the suffusion susceptibility classification proposed by Marot et al., 2016), between 3.03 and 3.09 for tests C (moderately erodible), between 2.93 and 2.98 for tests B90 (erodible), and I_α is equal to 2.94 for tests R90 (erodible). On the contrary, if the test is stopped before the stabilization of the hydraulic conductivity, the interpretation can lead to a higher

value of erosion resistance index and thus an overestimation of the soil resistance. This shows the necessity to perform suffusion tests by increasing the applied hydraulic gradient in order to have the possibility to follow the development of all possible processes and to continue the test as far as hydraulic conductivity becomes constant. The comparison of erosion resistance index obtained for tests B90 and B97 on one hand, and for tests R90 and R97 on the other hand permits to highlight the positive influence of density on soil resistance face suffusion process (both soils are erodible with initial dry density of 17.39kN/m^3 and moderately erodible with initial dry density of 18.74kN/m^3). These results are in good agreement with the results obtained by Indraratna et al. (2015) who showed that the increase of relative density permits to transform unstable specimens into stable ones. By considering tests characterized by a constant final hydraulic conductivity, it can also be noted that for soils B, C and R the erosion resistance index is between 2.93 and 3.64, whereas it reaches 4.65 for test A-b (corresponding suffusion susceptibility classification: moderately resistant). Thus soil A which contains less fine particles (initial fine content: 20%) appears more resistant than soils B (initial fine content: 25%), C and R (initial fine content about 29%). Thanks to the aforementioned interpretation of post-test grading, it is possible to conclude that the higher resistance of soil A is mainly due to the raise of filtration in specimen downstream part.

Finally even if tested soils were unstable according to grain size distribution based criteria, the suffusion susceptibility classification for tested specimens is between erodible (B90-a, R90-a and R90-b) and moderately resistant (A).

Recommendations for testing

According to the aforementioned results, several recommendations can be drawn to perform suffusion tests.

1. Even if grain size distribution based criteria lead to internally unstable state for all studied soils, a gradation of soil suffusion susceptibility can be obtained according to slight variations of initial soil grading and density. Thus suffusion tests have to be performed.
2. Suffusion is the result of the combination of three processes: detachment, transport and filtration, which in particular depend on history of hydraulic loading. With the objective to follow the development of all possible combinations, tests must be realized by increasing the applied hydraulic gradient and it should be carried on until the stabilization of the hydraulic conductivity.
3. The hydraulic loading on one hand, and the induced erosion on the other hand must be independently characterized. Thus the energy dissipated by the water seepage, E_{flow} and the cumulative loss dry mass are computed respectively. Finally at the end of each test, which corresponds to the invariability of the hydraulic conductivity, the erosion sensibility classification can be evaluated by the value of the erosion resistance index.

CONCLUSION

The characterization of suffusion susceptibility is an important issue for contributing to the safety assessment of hydraulic earth structures. Tests realized under different hydraulic loading histories highlight the complexity of suffusion which can be understood as the process by which the finest soil particles are detached and

transported within the porous soil network. Detached particles can be filtered out with an increasing rate depending on initial gradation, density and evolution of hydraulic loading.

According to the type of hydraulic loading, the predominant process can be either filtration or erosion. Thus even if a transport of particles is geometrically possible, the action of hydraulic loading must be studied.

The analysis of the suffusion onset can be carried out by determining the critical hydraulic gradient. However, the realized study shows that the type of hydraulic loading can substantially modify the value of critical hydraulic gradient at which suffusion occurs. For other erosion processes, the interpretative method can consist in describing the erosion rate by using the excess shear stress equation. In the case of suffusion, the influence of the hydraulic loading history on the erosion coefficient value and the weak values of correlation coefficient show that such approach does not permit to determine a unique suffusion susceptibility characterization.

A new interpretative method is proposed, linking the cumulative eroded dry mass to the energy dissipated by the fluid flow. This method is efficient to determine the suffusion susceptibility for cohesionless material. This study also shows the necessity to perform suffusion tests by increasing the applied hydraulic gradient and to continue tests until hydraulic conductivity becomes constant.

ACKNOWLEDGEMENT

The authors thank the Indonesian Directorate General of Higher Education (DIKTI), the Sultan Agung Islamic University Indonesia, the Ministry of Education and Training of Vietnam and the University of Danang Vietnam, the company IMSRN France, for providing financial support for this work.

REFERENCES

Bendahmane, F., Marot, D. and Alexis, A. (2008). "Experimental parametric Study of Suffusion and Backward Erosion." *J. Geotech. Geoenviron. Eng.,* 134(1), 57-67.

Chang, D.S. and Zhang, L.M. (2011). "A Stress-controlled erosion apparatus for studying internal erosion in soils." *J. ASTM Geotech Test.*, 34(6), 579-589

Chang, D.S. and Zhang, L.M. (2013). "Extended internal stability criteria for soils under seepage." *Soils Found.,* 53(4), 569-583.

Fell, R. and Fry ,J.J. (eds) (2007). "Internal erosion of dams and their foundations." Taylor & Francis, London.

Fell, R. and Fry, J.J. (2013). "Erosion in geomechanics applied to dams and levees." 1-99. Bonelli S. Editor. ISTE – Wiley.

Fry, J.J., Vogel, A., Royet, P. and Courivaud, J.R. (2012). "Dam failures by erosion: lessons from ERINOH data bases." *Proc. 6th Int. Conference on Scour and Erosion (ICSE-6)*, 27-31 August, Paris, France, 273-280.

Indraratna, B., Israr J. and Rujikiatkamjorn, C. (2015). "Geometrical method for evaluating the internal instability of granular filters based on constriction size distribution." *J. Geotech. Geoenviron. Eng.,* 141(10), 04015045.

Ke, L. and Takahashi, A. (2012). "Strength reduction of cohesionless soil due to internal erosion induced by one dimensional upward seepage flow." *Soils Found.,* 52(2012), 698–711.

Ke, L., and Takahashi, A. (2014). "Triaxial erosion test for evaluation of mechanical consequences of internal erosion." *Geotech. Test. J.*, 37(2), 20130049.

Ke, L. and Takahashi, A. (2015). "Drained monotonic responses of suffusional cohesionless soils." *J. Geotech. Geoenviron. Eng.,* 141(8), 04015033.

536 Kenney, T.C. and Lau, D. (1985). “Internal stability of granular filters”. *Can. Geotech.*
537 *J.,* 22, 215-225.
538 Li, M. and Fannin, J. (2008). “Comparison of two criteria for internal stability of granular
539 soil.” *Can. Geotech. J.,* 45, 1303-1309.
540 Luo, Y.L., Qiao, L., Liu, X.X., Zhan, M.L. and Sheng, J.C. (2013). “Hydro-mechanical
541 experiments on suffusion under long-term large hydraulic heads.” *Nat. Hazards*,
542 65, 1361–1377.
543 Marot, D., Bendahmane, F., Rosquoët, F. and Alexis, A. (2009). “Internal flow effects
544 on isotropic confined sand-clay mixtures.” *Soil & Sediment Contamination, an*
545 *International Journal,* 18(3), 294-306.
546 Marot, D., Bendahmane, F. and Konrad, J.M. (2011a). “Multi-channel optical sensor
547 to quantify particle stability under seepage flow.” *Can. Geotech. J.,* 48, 1772-1787.
548 Marot, D., Regazzoni, P.L. and Wahl, T. (2011b). “Energy based method for providing
549 soil surface erodibility rankings.” *J. Geotech. Geoenviron. Eng.,* 137(12), 1290-
550 1294.
551 Marot, D., Bendahmane, F. and Nguyen, H.H. (2012). “Influence of angularity of
552 coarse fraction grains on internal erosion process.” *La Houille Blanche,*
553 *International Water Journal,* 6, 47-53.
554 Marot, D., Rochim, A., Nguyen, H.H., Bendahmane, F. and Sibille L. (2016).
555 “Assessing the susceptibility of gap graded soils to internal erosion: proposition of
556 a new experimental methodology.” *Nat. Hazards*, Volume 83, Issue 1, pp 365-388.
557 Moffat, R. and Fannin, J. (2006). “A large permeameter for study of internal stability in
558 cohesionless soils.” *J. ASTM Geotech Test.,* 29(4), 273-279.

559 Nguyen, H.H. (2012). “Caractérisation de mécanismes d’érosion interne: confrontation
560 d’érodimètres et d’approches.” Ph.D. Thesis. Université de Nantes.
561 Nguyen, H.H., Marot, D. and Bendahmane, F. (2012). “Erodibility characterisation for
562 suffusion process in cohesive soil by two types of hydraulic loading.” *La Houille*
563 *Blanche, International Water Journal,* 6, 54-60.
564 Reddi, L.N., Lee, I. and Bonala, M.V.S. (2000). “Comparison of internal and surface
565 erosion using flow pump test on a sand-kaolinite mixture.” *J. ASTM Geotech Test.,*
566 23(1), 116-122.
567 Sibille, L., Marot, D. and Sail, Y. (2015a). “A description of internal erosion by suffusion
568 and induced settlements on cohesionless granular matter.” *Acta Geotechnica*, 10,
569 735-748.
570 Sibille, L., Lominé, F., Poullain, P., Sail, Y. and Marot, D. (2015b). “Internal erosion in
571 granular media: direct numerical simulations and energy interpretation.” *Hydrol.*
572 *Processes*, 29(9), 2149-2163.
573 Skempton, A.W. and Brogan, J.M. (1994). “Experiments on piping in sandy gravels.”
574 *Géotechnique,* 44(3), 440-460.
575 U.S. Army Corps of Engineers (1953). “Filter experiments and design criteria.”
576 *Technical Memorandum* No. 3-360, Waterways Experiment Station, Vicksburg.
577 Wan, C.F. and Fell, R. (2004). “Investigation of rate of erosion of soils in embankment
578 dams.” *J. Geotech. Geoenviron. Eng.,* 130(4), 373-380.
579 Wan, C.F. and Fell, R. (2008). “Assessing the potential of internal instability and
580 suffusion in embankment dams and their foundations.” *J. Geotech. Geoenviron.*
581 *Eng* 134(3); 401-407.

FIGURE CAPTIONS

Fig. 1 Sketch of the experimental bench

Fig. 2 Grain size distribution of tested soils

Fig. 3 Time evolution of multi-staged and single staged hydraulic gradients

Fig. 4 Time evolution of hydraulic conductivity, soils A and R, hydraulic loadings a and b

Fig. 5 Time evolution of hydraulic conductivity, soils B and C, hydraulic loadings a and b. Identification of predominant processes during test B90-a

Fig. 6 Time evolution of hydraulic conductivity, tests A-c, B90-c, B90-q2, B90-k, and R97-q1

Fig. 7 Time evolution of erosion rate, tests B90-a, B90-c and B90-q2

Fig. 8 Initial soil gradation and gradations of upstream and downstream parts after suffusion test for (a) test A-a; (b) test B90-a

Fig. 9 Flow velocity versus hydraulic gradient, critical hydraulic gradient, soil B

Fig. 10 Erosion rate versus hydraulic shear stress, soil A

Fig. 11 Cumulative loss dry mass versus cumulative expended energy, soil A

Fig. 12 Cumulative loss dry mass versus cumulative expended energy, tests B90-a, B90-c, B90-k and B90-q2

600 **Fig. 13** Cumulative loss dry mass versus cumulative expended energy, tests B97-a,
601 B97-b, C-a and C-b

602 **Fig. 14** Cumulative loss dry mass versus cumulative expended energy, soil R

603

604

605

606 **Table 1** Properties of tested gradations

	Tested gradations			
Properties	A	B	C	R
P (%)	1.227	1.533	1.779	1.200
G_r	3.2	3.2	4	WG
C_u	17.06	19.52	21.07	24.46
d_{15}/d_{85}	8.761	8.741	8.724	9.653
$(H/F)_{min}$	0.038	0.035	0.033	0.165
D $(H/F)_{min}$ (mm)	0.400	0.400	0.400	0.212
$D_{c35}^{c}/d_{85,SA}^{f}$	3.295	3.295	3.295	2.903

607

608 P : percentage of particle smaller than 0.063mm; $G_r = d_{max}/d_{min}$ (d_{max} and d_{min}: maximal
609 and minimal particle sizes characterizing the gap in the grading curve); C_u: uniformity
610 coefficient; d_{15} and d_{85} are the sieve sizes for which 15% and 85% respectively of the
611 weighed soil is finer; F and H are the mass percentages of the grains with a size, lower
612 than a given particle diameter d and between d and 4d respectively; D $(H/F)_{min}$ is the
613 corresponding diameter with the minimum value of ratio H/F ; D_{c35}^{c} is the controlling
614 constriction for coarser fraction from constriction size distribution by surface area
615 technique; $d_{85,SA}^{f}$ is the representative size for finer fraction by surface area technique;
616 WG: widely graded soil.

617

618 **Table 2** Properties of tested specimens

619

Soil reference in paper	Specimen reference in paper	Initial dry density γ_d (kN/m^3)	Applied hydraulic gradient i	Injected flow q (ml/min)	Test duration (min)
A	A-a	17.39	From 0.1 to 15	-	270
	A-a_rep	17.39	From 0.1 to 15	-	250
	A-b	17.39	From 1 to 13	-	130
	A-c	17.39	4	-	300
B	B90-a	17.39	From 0.1 to 6	-	180
	B90-c	17.39	4	-	300
	B90-k	17.39	From 0.5 to 1	-	1440
	B90-q2	17.39	-	1.641	270
	B97-a	18.74	From 0.1 to 12	-	240
	B97-b	18.74	From 1 to 9	-	90
C	C-a	18.74	From 0.1 to 9	-	210
	C-b	18.74	From 1 to 7	-	70
R	R90-a	17.39	From 0.1 to 6	-	180
	R90-b	17.39	From 1 to 8	-	80
	R97-b	18.74	From 1 to 12	-	120
	R97-q1	18.74	-	1.247	210

620 **Table 3** Critical hydraulic gradient, multi staged hydraulic gradient conditions

Tested specimens	Critical hydraulic gradient i_c	
	Hydraulic loading (a)	Hydraulic loading (b)
A	3.5 – 3.9	4.5
B90	1.5	
B97	0.5	2
C	2.5	2.5
R90	0.6	1.8
R97		3.4

621

622 **Table 4** Erosion coefficient and correlation coefficient, multi staged hydraulic gradient

623 conditions

Tested specimens	Hydraulic loading (a)		Hydraulic loading (b)	
	Erosion coefficient k_d (s/m)	Correlation coefficient R^2	Erosion coefficient k_d (s/m)	Correlation coefficient R^2
A	10^{-8} - 9 10^{-9}	0.77-0.59	3 10^{-8}	0.23
B90	10^{-6}	0.54		
B97	4 10^{-7}	0.01	7 10^{-7}	0.05
C	6 10^{-7}	0.08	10^{-6}	0.04
R90	8 10^{-7}	0.15	2 10^{-6}	0.06
R97			2 10^{-7}	0.02

624
625

626

627 **Table 5** Erosion resistance index

Tested specimens	Erosion resistance index I_α (-)				
	Hydraulic loading (a)	Hydraulic loading (b)	Hydraulic loading (c)	Hydraulic loading (k)	Hydraulic loading (q1 - q2)
A	5.06 – 5.12	**4.65**	5.00		
B90	**2.93**		3.25	**2.98**	3.47
B97	**3.64**	**3.40**			
C	**3.03**	**3.09**			
R90	**2.94**	**2.94**			
R97		**3.52**			3.29

Rochim A., Marot D., Sibille L., Le V.T. (2017). Effect of hydraulic loading history on the characterization of suffusion susceptibility of cohesionless soils. Journal of Geotechnical and Geoenvironmental Engineering (ASCE), 143(7). DOI 10.1061/(ASCE)GT.1943-5606.0001673

Figure 1

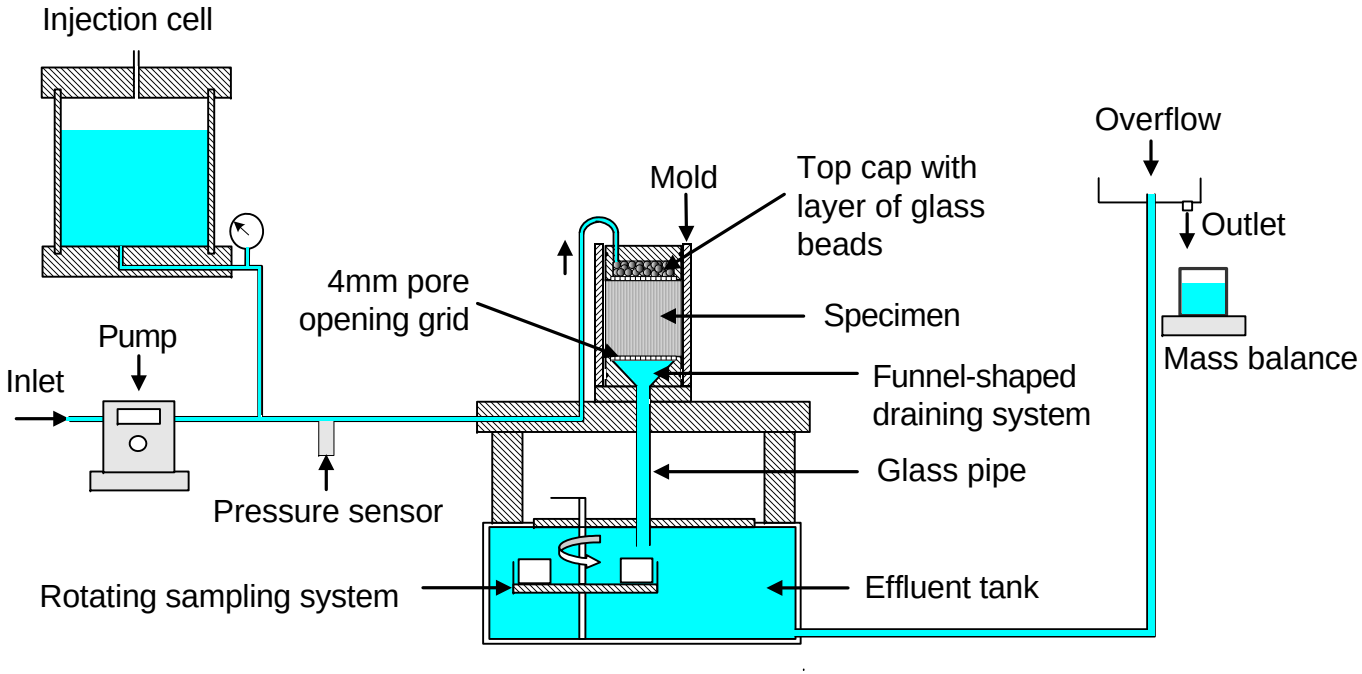

Rochim A., Marot D., Sibille L., Le V.T. (2017). Effect of hydraulic loading history on the characterization of suffusion susceptibility of cohesionless soils. Journal of Geotechnical and Geoenvironmental Engineering (ASCE), 143(7). DOI 10.1061/(ASCE)GT.1943-5606.0001673

Figure 2

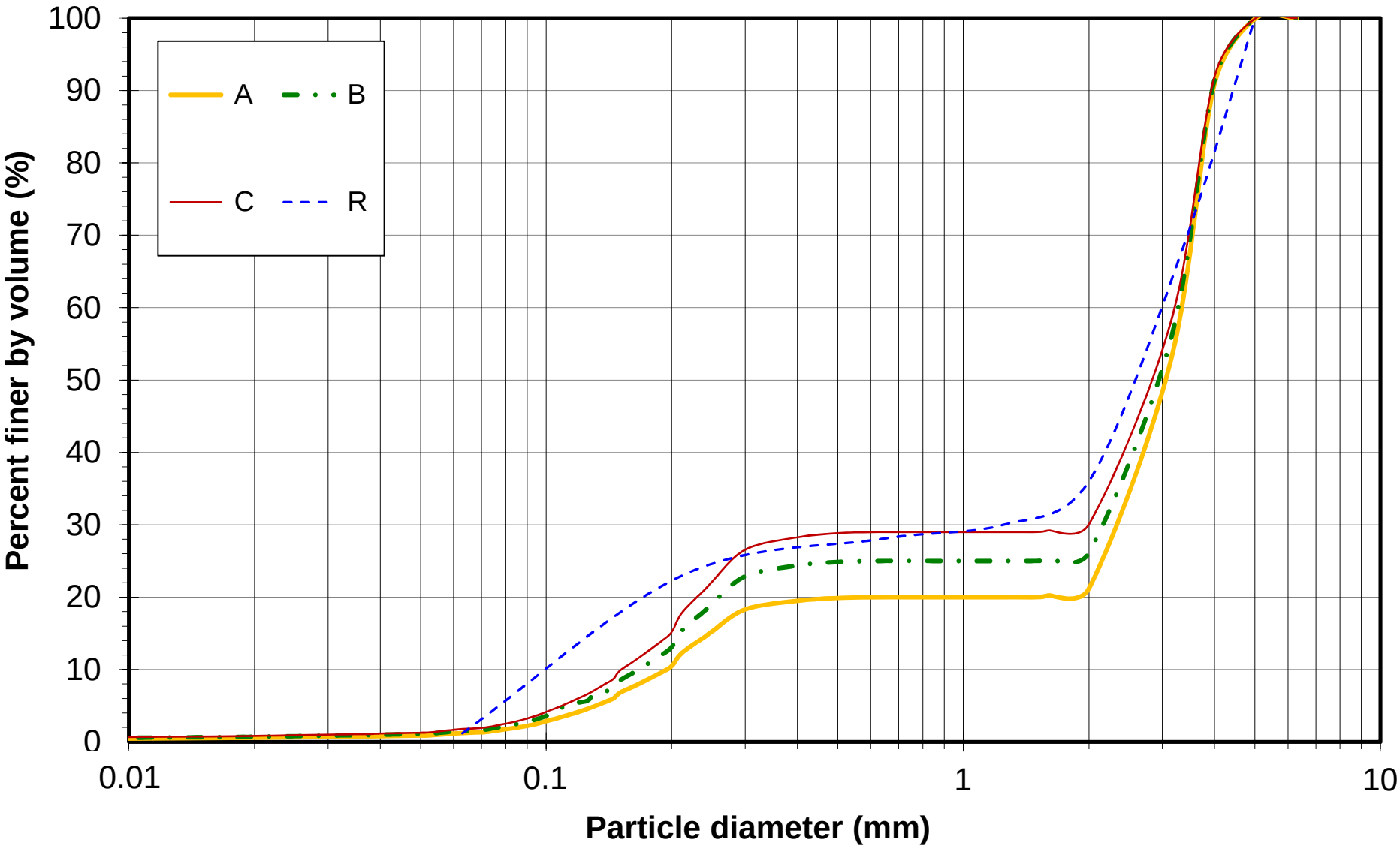

Rochim A., Marot D., Sibille L., Le V.T. (2017). Effect of hydraulic loading history on the characterization of suffusion susceptibility of cohesionless soils. Journal of Geotechnical and Geoenvironmental Engineering (ASCE), 143(7). DOI 10.1061/(ASCE)GT.1943-5606.0001673

Figure 3

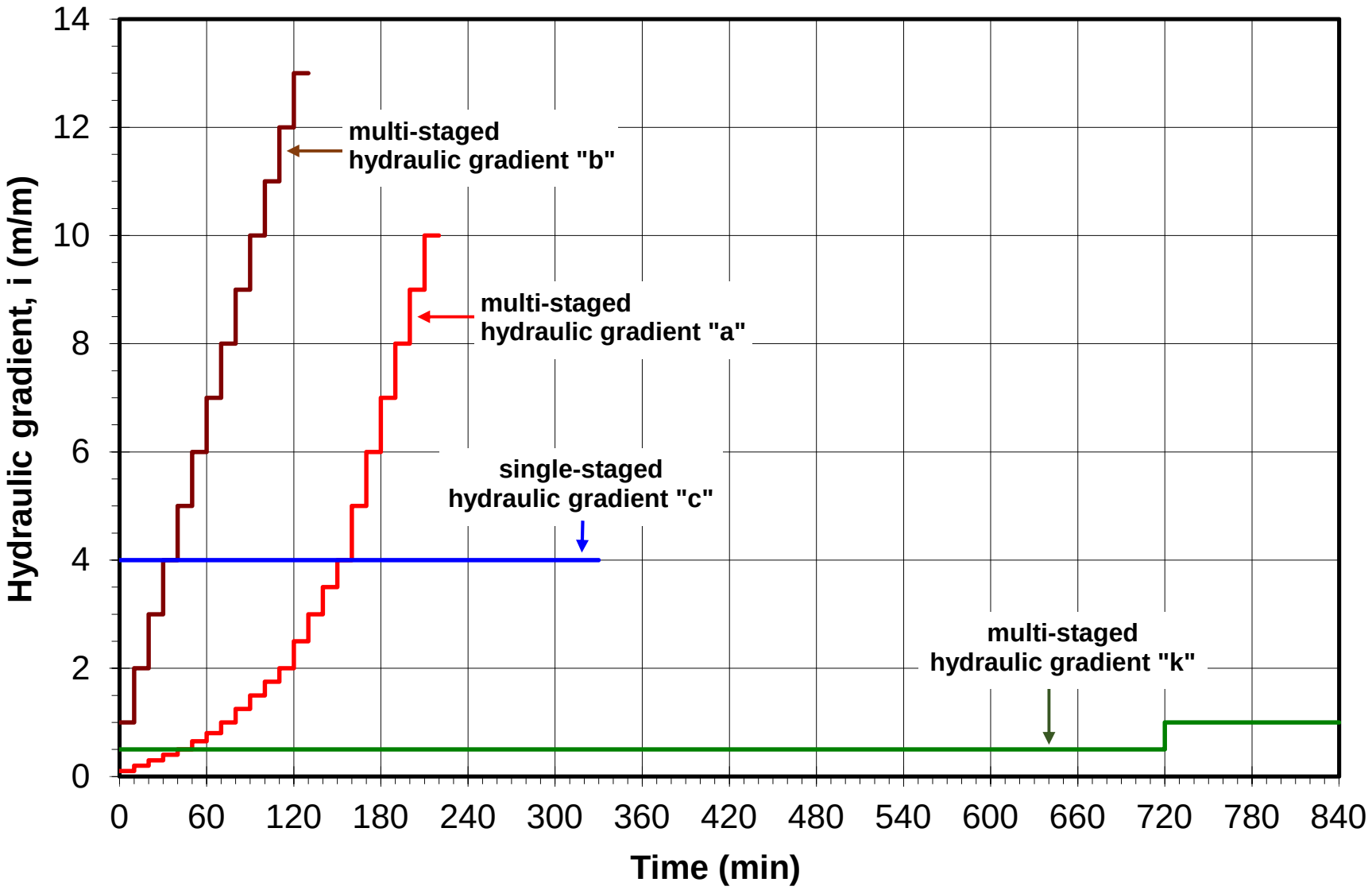

Rochim A., Marot D., Sibille L., Le V.T. (2017). Effect of hydraulic loading history on the characterization of suffusion susceptibility of cohesionless soils. Journal of Geotechnical and Geoenvironmental Engineering (ASCE), 143(7). DOI 10.1061/(ASCE)GT.1943-5606.0001673

Figure 4

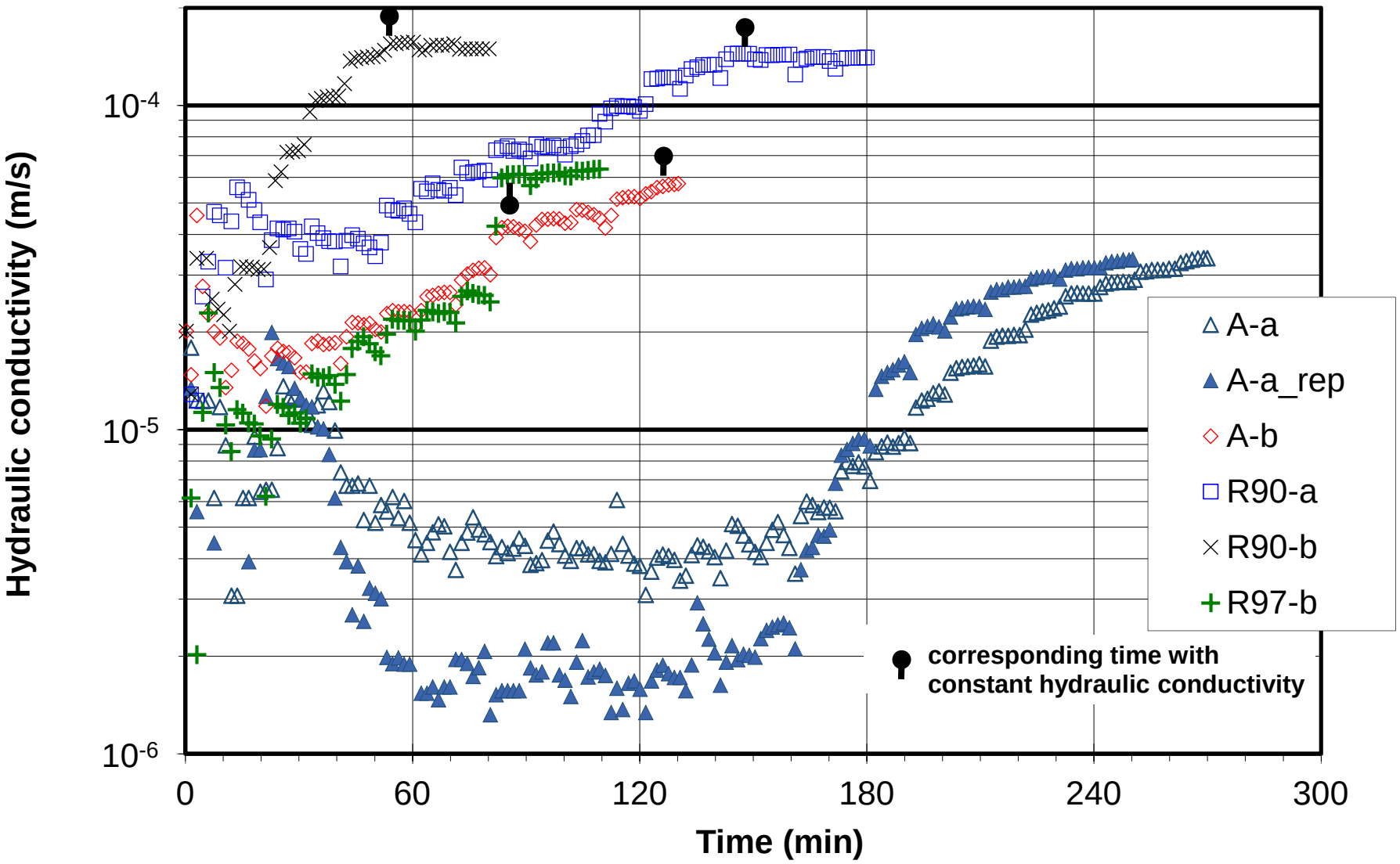

Rochim A., Marot D., Sibille L., Le V.T. (2017). Effect of hydraulic loading history on the characterization of suffusion susceptibility of cohesionless soils. Journal of Geotechnical and Geoenvironmental Engineering (ASCE), 143(7). DOI 10.1061/(ASCE)GT.1943-5606.0001673

Figure 5

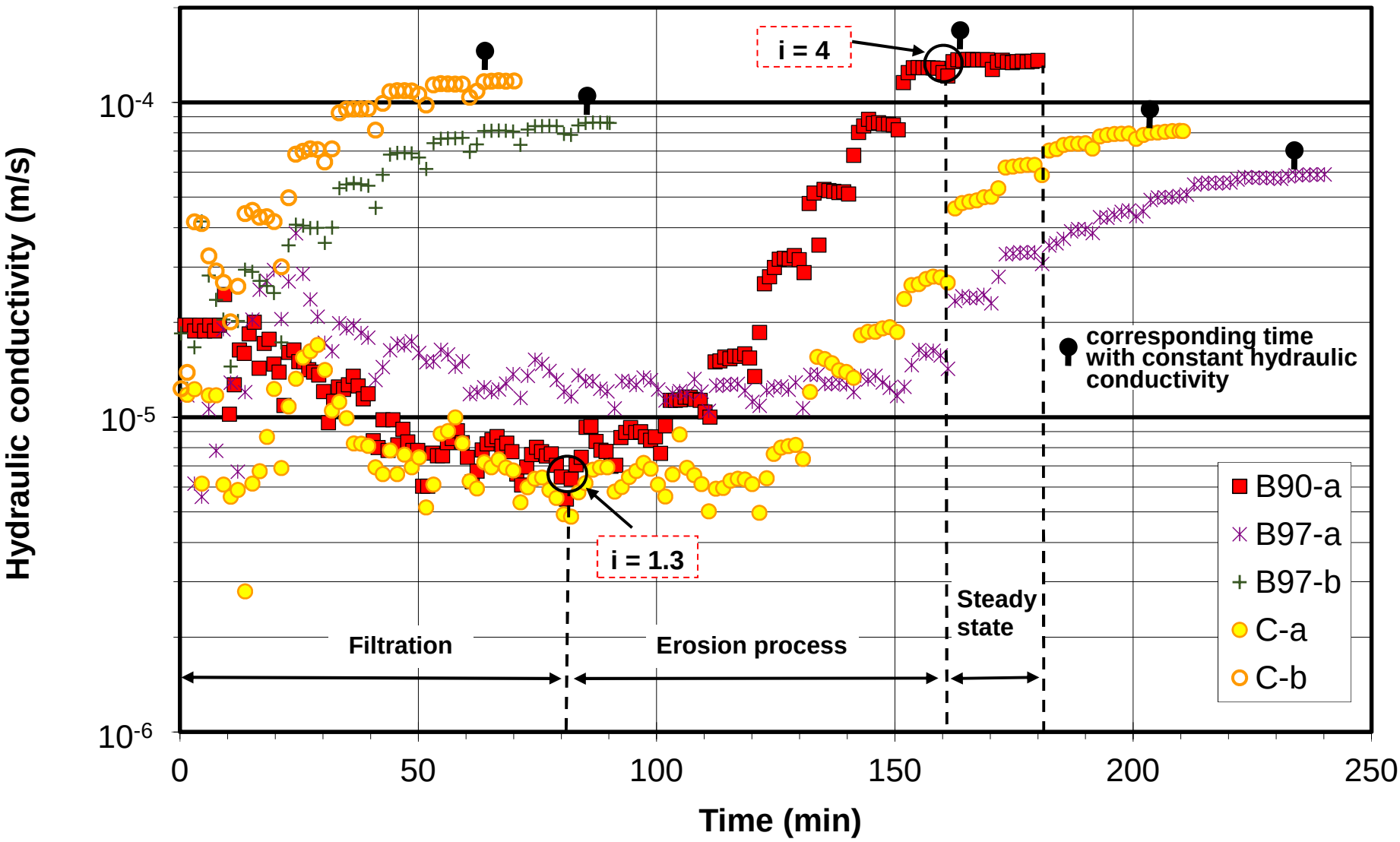

Rochim A., Marot D., Sibille L., Le V.T. (2017). Effect of hydraulic loading history on the characterization of suffusion susceptibility of cohesionless soils. Journal of Geotechnical and Geoenvironmental Engineering (ASCE), 143(7). DOI 10.1061/(ASCE)GT.1943-5606.0001673

Figure 6

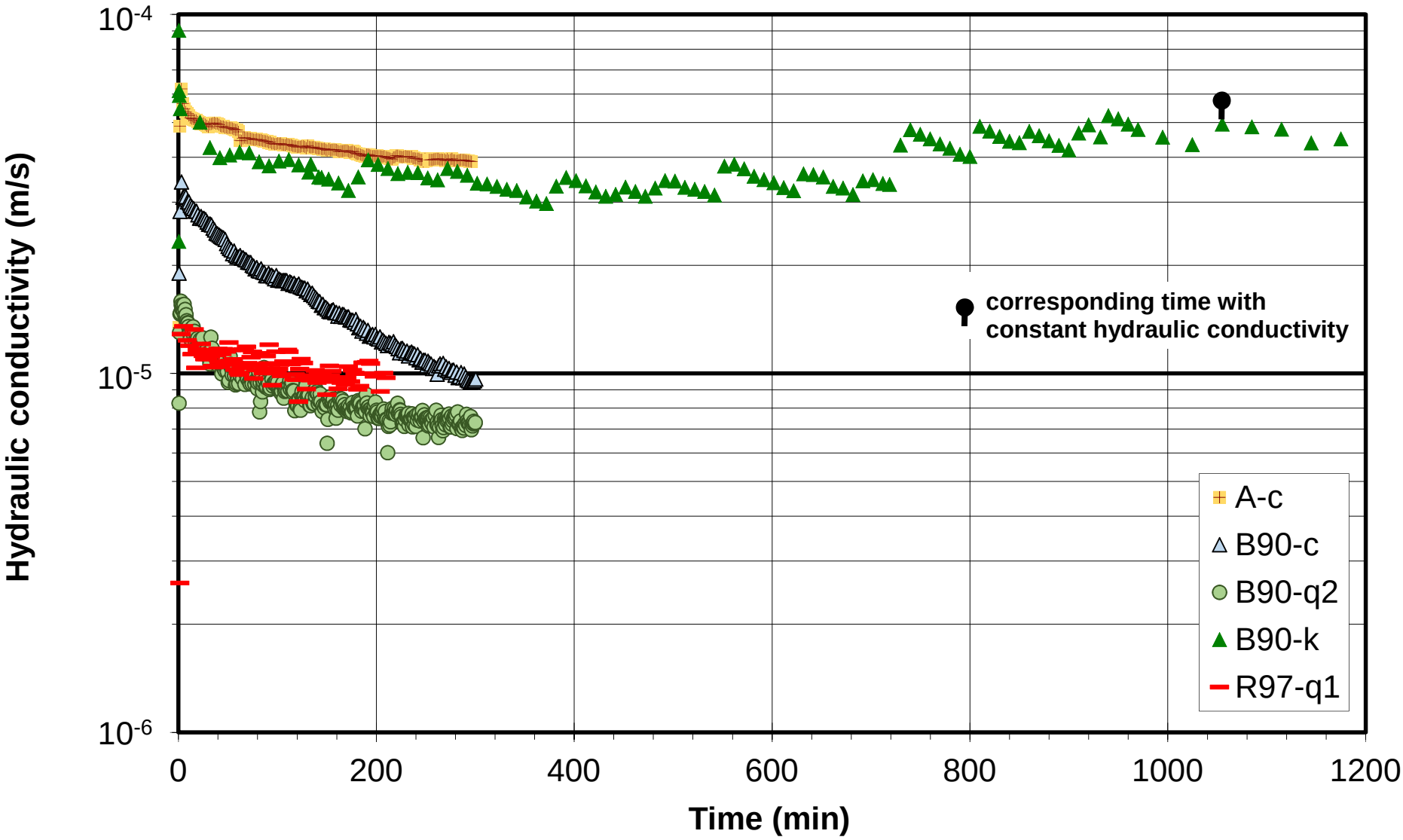

Rochim A., Marot D., Sibille L., Le V.T. (2017). Effect of hydraulic loading history on the characterization of suffusion susceptibility of cohesionless soils. Journal of Geotechnical and Geoenvironmental Engineering (ASCE), 143(7). DOI 10.1061/(ASCE)GT.1943-5606.0001673

Figure 7

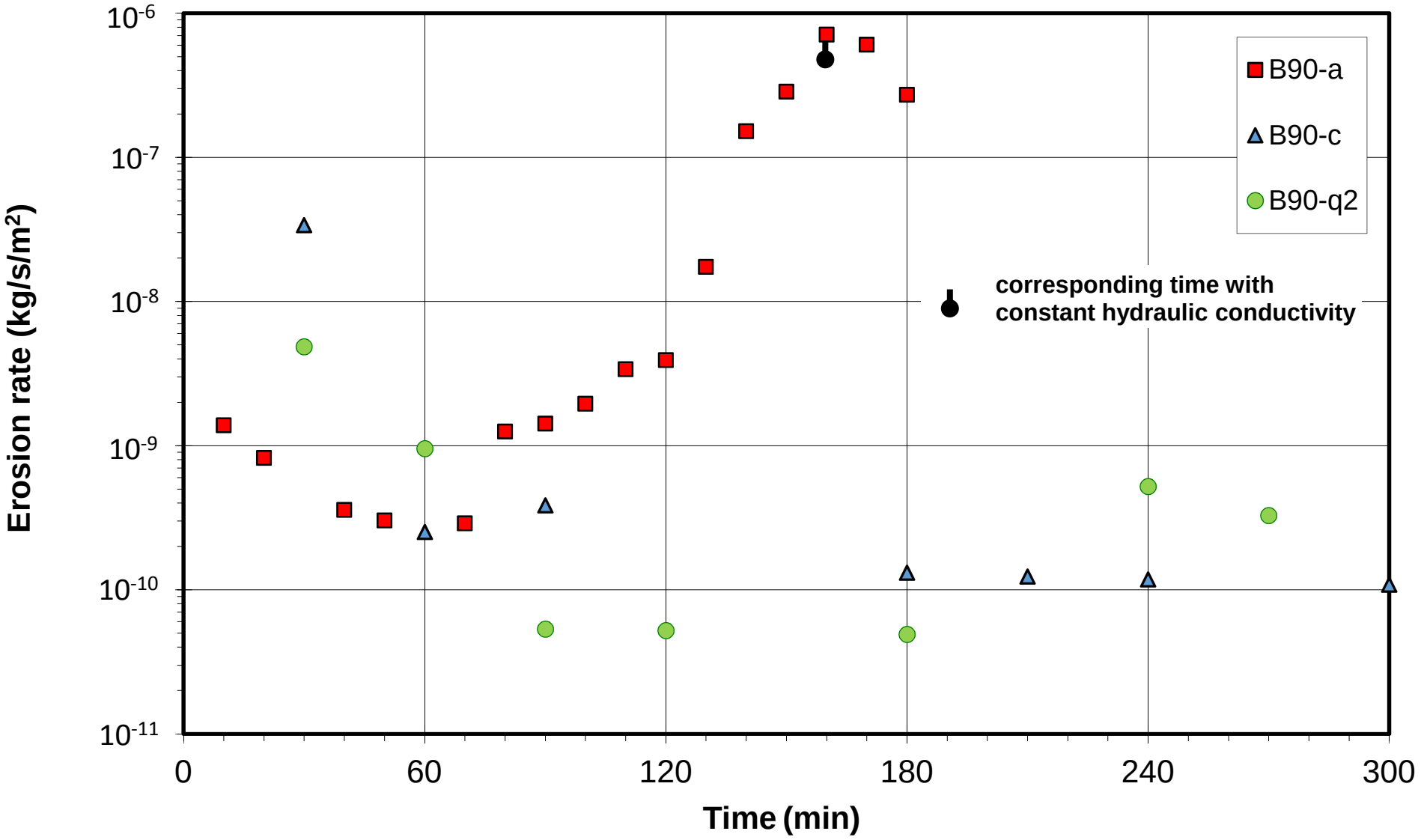

Rochim A., Marot D., Sibille L., Le V.T. (2017). Effect of hydraulic loading history on the characterization of suffusion susceptibility of cohesionless soils. Journal of Geotechnical and Geoenvironmental Engineering (ASCE), 143(7). DOI 10.1061/(ASCE)GT.1943-5606.0001673

Figure 8a

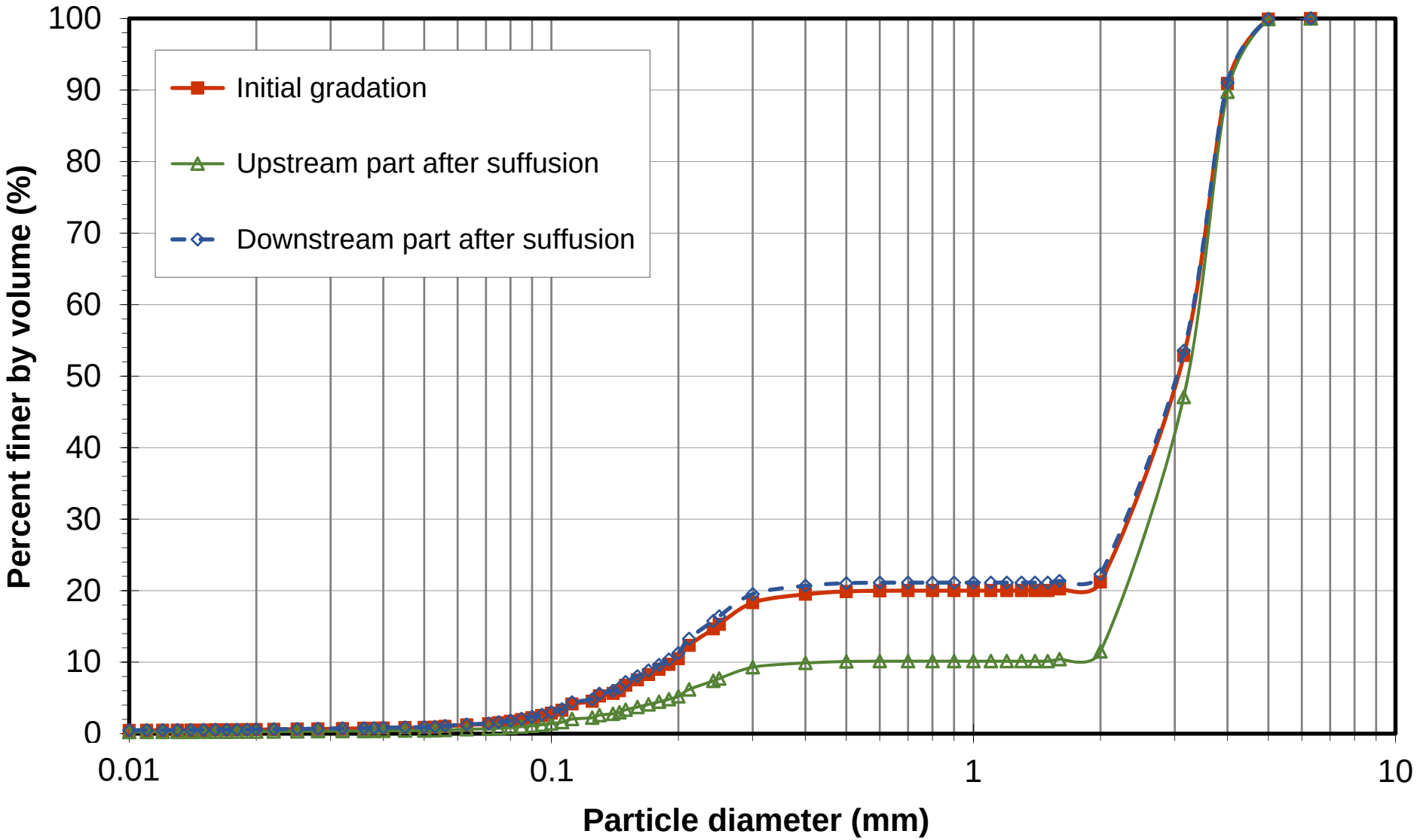

Rochim A., Marot D., Sibille L., Le V.T. (2017). Effect of hydraulic loading history on the characterization of suffusion susceptibility of cohesionless soils. Journal of Geotechnical and Geoenvironmental Engineering (ASCE), 143(7). DOI 10.1061/(ASCE)GT.1943-5606.0001673

Figure 8b

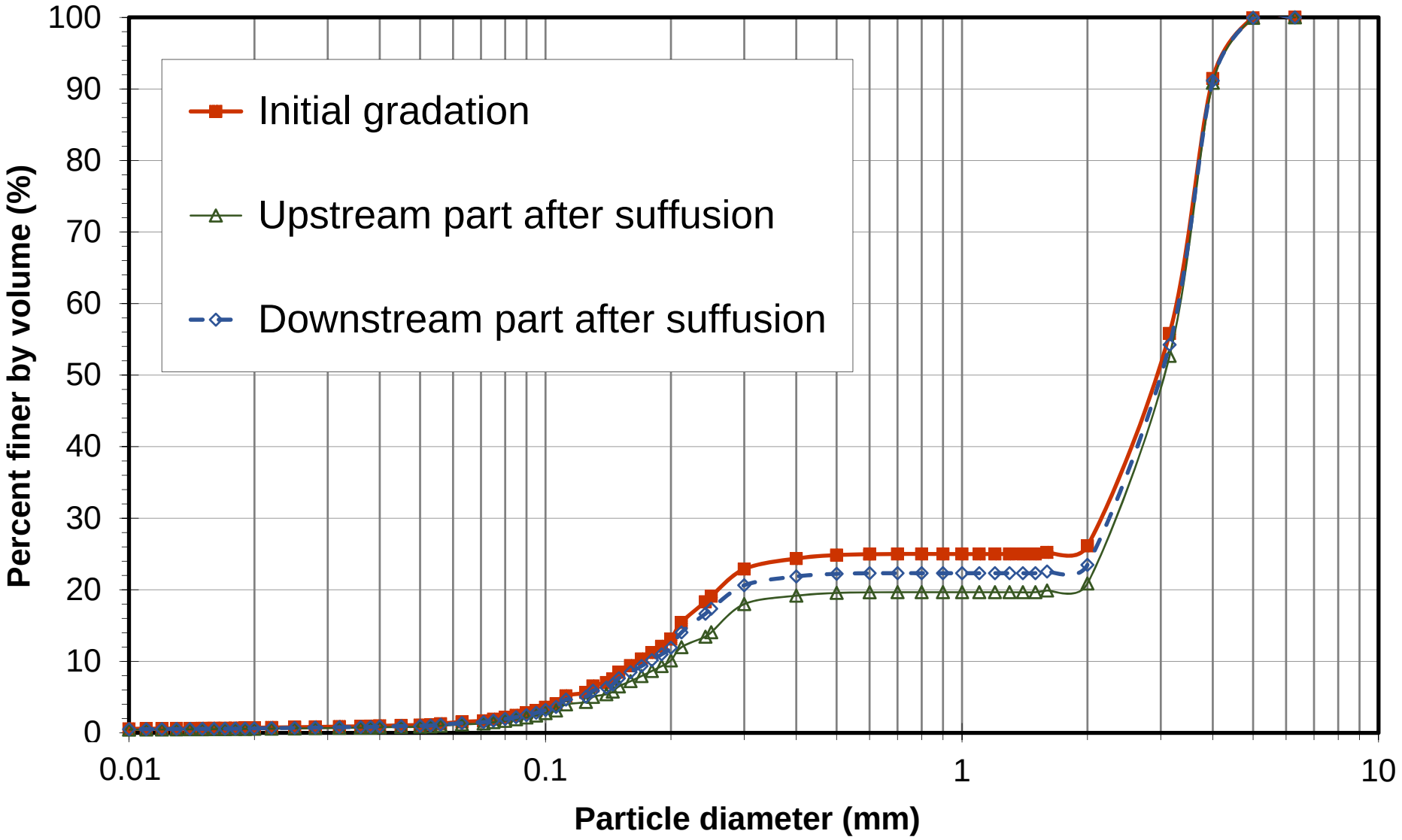

Rochim A., Marot D., Sibille L., Le V.T. (2017). Effect of hydraulic loading history on the characterization of suffusion susceptibility of cohesionless soils. Journal of Geotechnical and Geoenvironmental Engineering (ASCE), 143(7). DOI 10.1061/(ASCE)GT.1943-5606.0001673

Figure 9

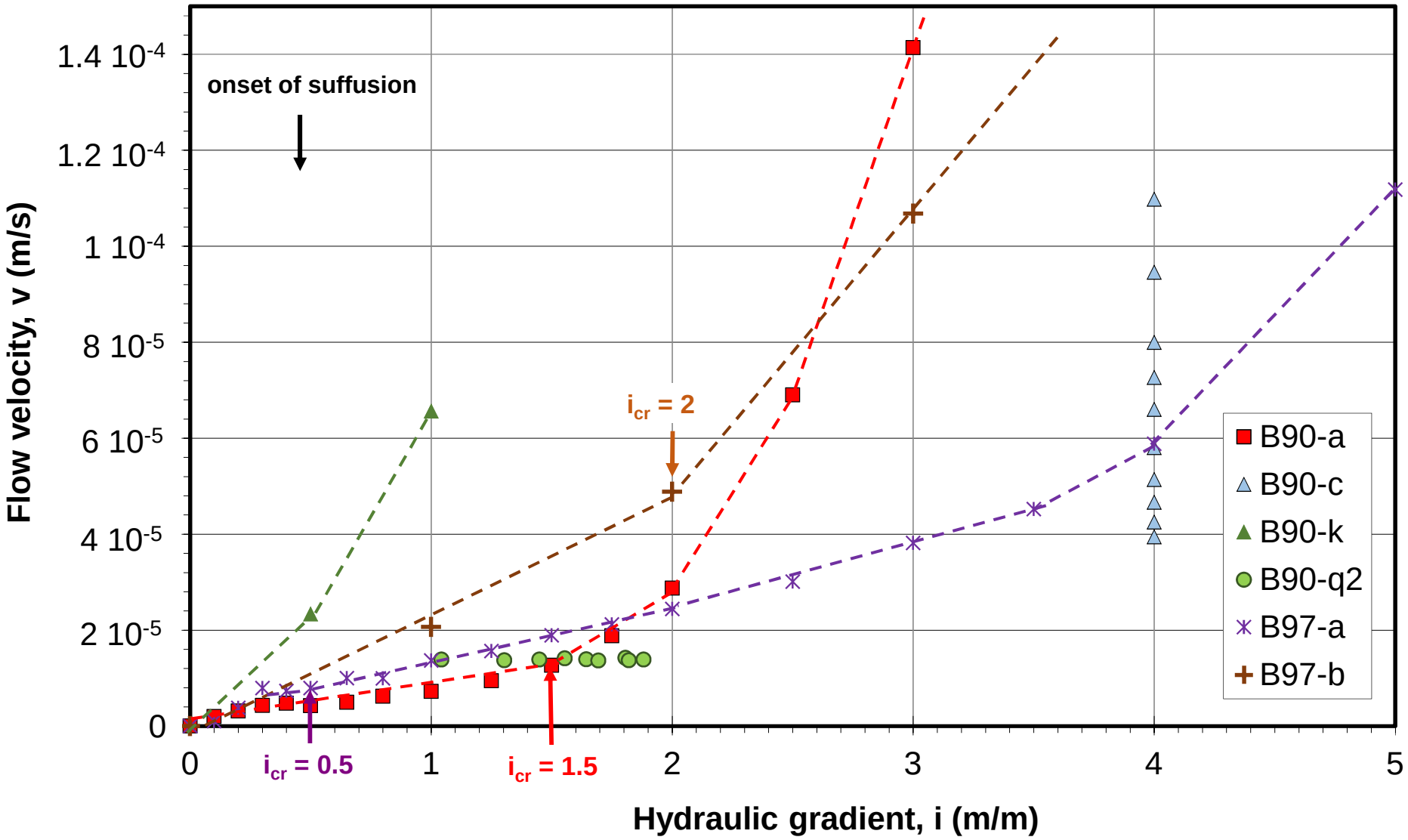

Rochim A., Marot D., Sibille L., Le V.T. (2017). Effect of hydraulic loading history on the characterization of suffusion susceptibility of cohesionless soils. Journal of Geotechnical and Geoenvironmental Engineering (ASCE), 143(7). DOI 10.1061/(ASCE)GT.1943-5606.0001673

Figure 10

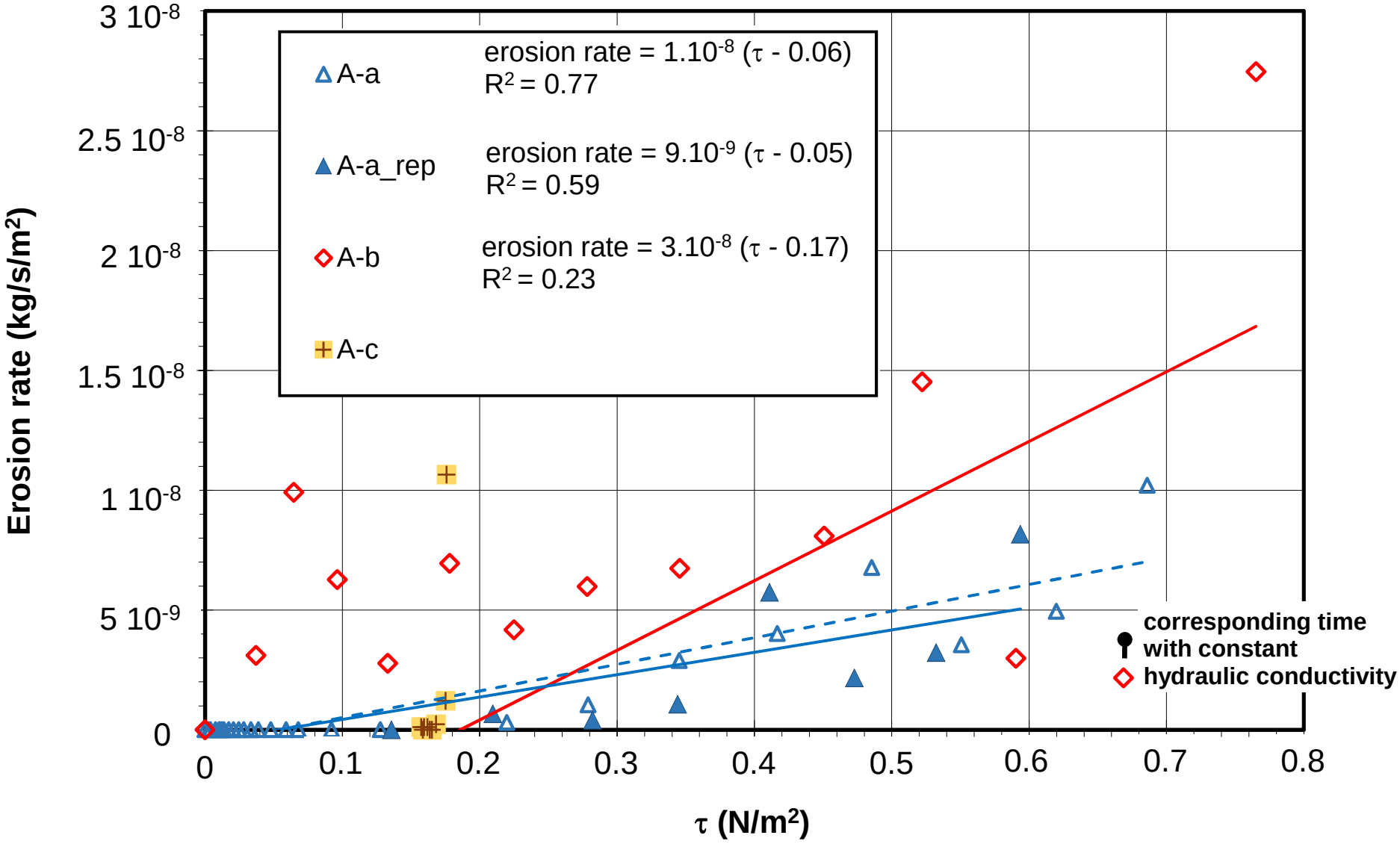

Rochim A., Marot D., Sibille L., Le V.T. (2017). Effect of hydraulic loading history on the characterization of suffusion susceptibility of cohesionless soils. Journal of Geotechnical and Geoenvironmental Engineering (ASCE), 143(7). DOI 10.1061/(ASCE)GT.1943-5606.0001673

Figure 11

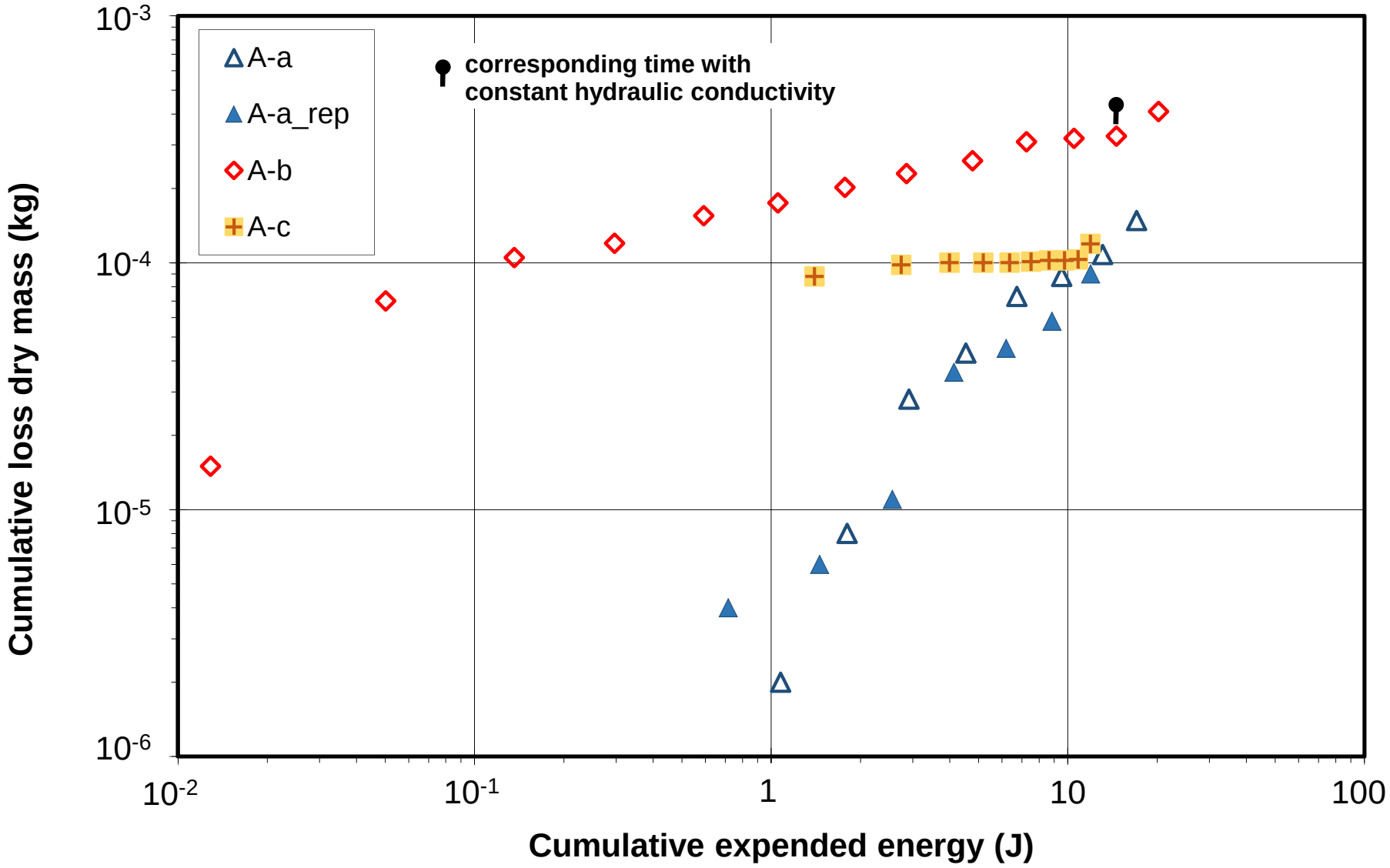

Rochim A., Marot D., Sibille L., Le V.T. (2017). Effect of hydraulic loading history on the characterization of suffusion susceptibility of cohesionless soils. Journal of Geotechnical and Geoenvironmental Engineering (ASCE), 143(7). DOI 10.1061/(ASCE)GT.1943-5606.0001673

Figure 12

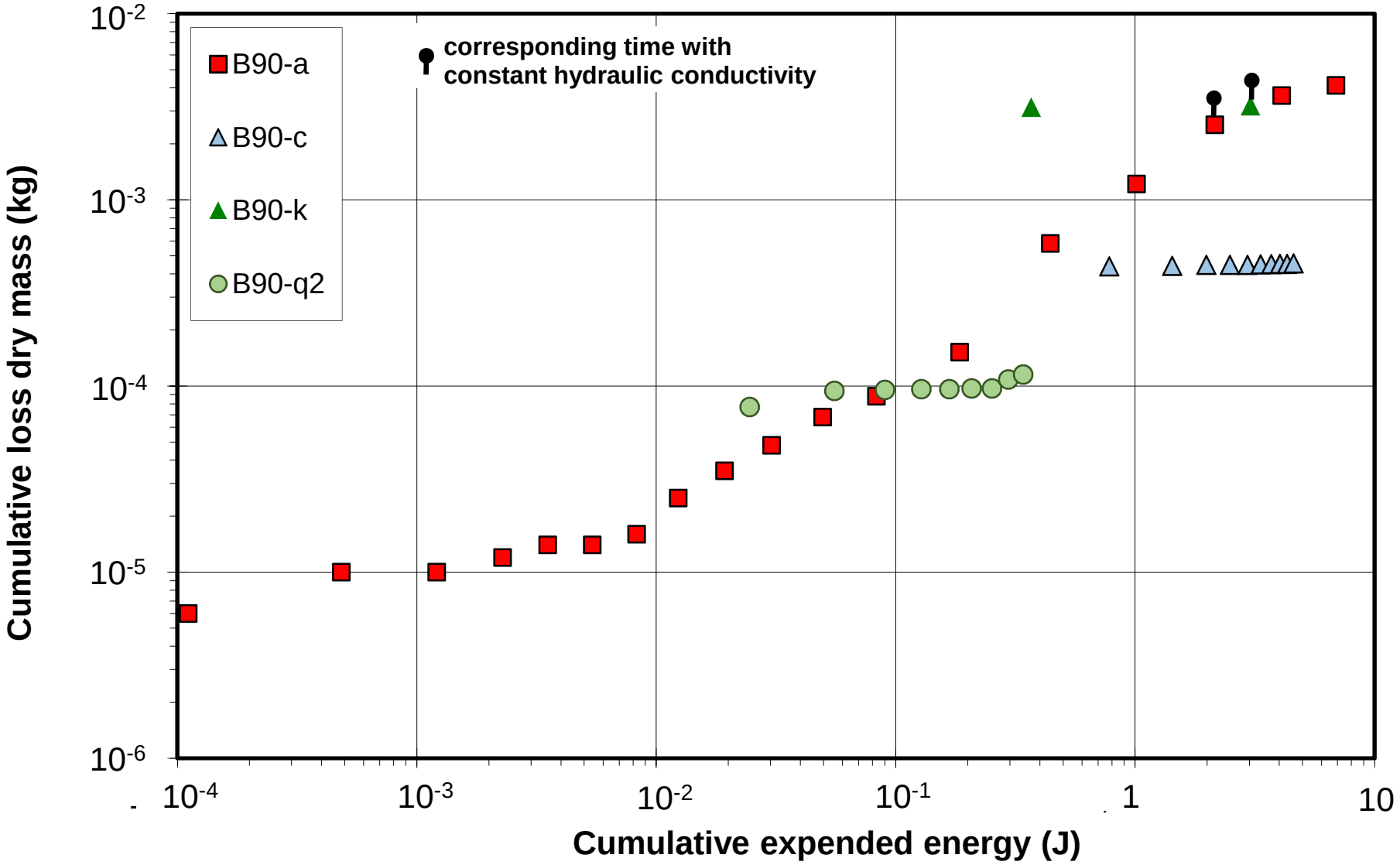

Rochim A., Marot D., Sibille L., Le V.T. (2017). Effect of hydraulic loading history on the characterization of suffusion susceptibility of cohesionless soils. Journal of Geotechnical and Geoenvironmental Engineering (ASCE), 143(7). DOI 10.1061/(ASCE)GT.1943-5606.0001673

Figure 13

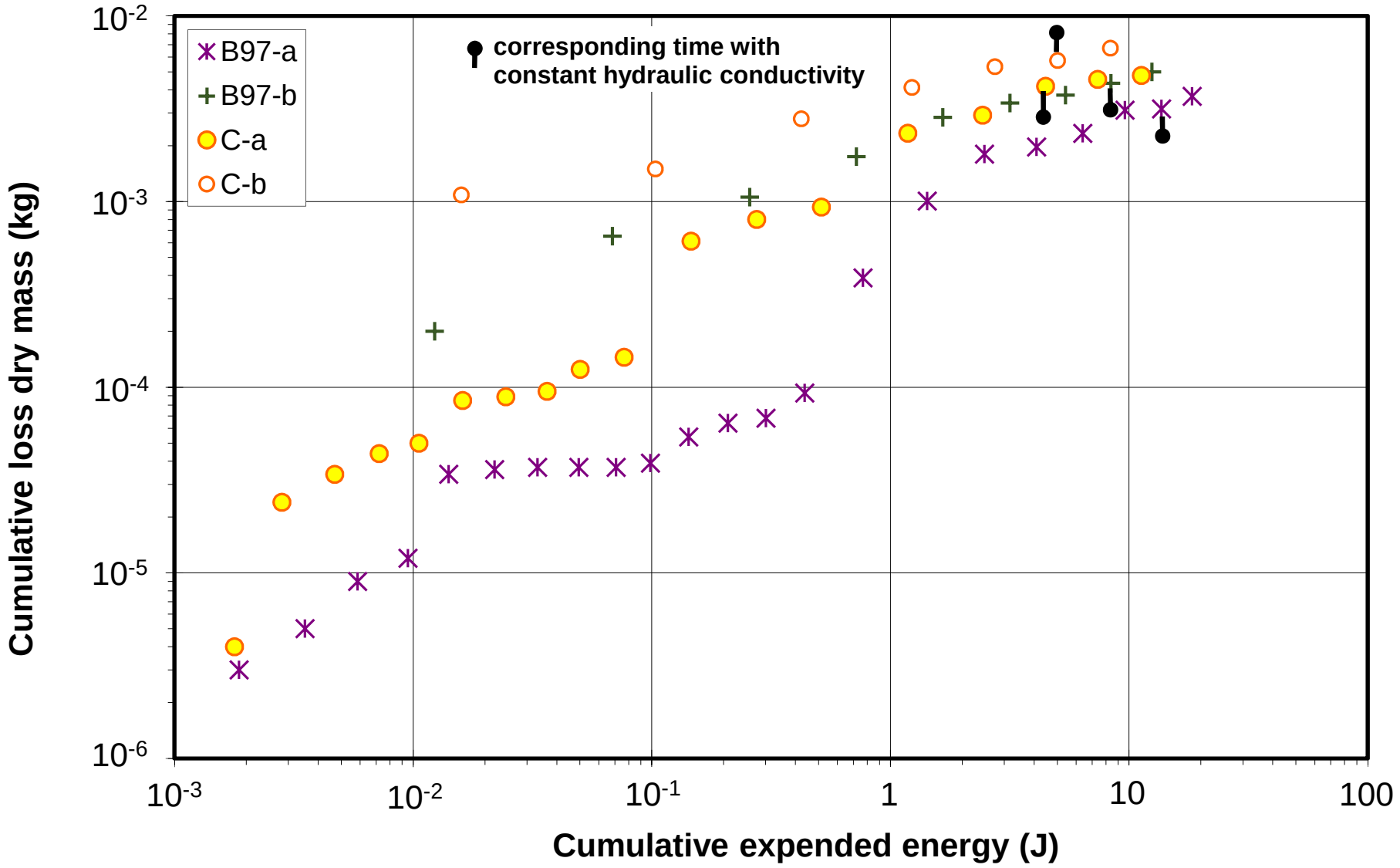

Rochim A., Marot D., Sibille L., Le V.T. (2017). Effect of hydraulic loading history on the characterization of suffusion susceptibility of cohesionless soils. Journal of Geotechnical and Geoenvironmental Engineering (ASCE), 143(7). DOI 10.1061/(ASCE)GT.1943-5606.0001673

Figure 14